南京航空航天大学

论文集

（二〇〇一年）

第1册

一院

南京航空航天大学科技部编

二〇〇二年六月

一　院

○一一～○一二系

目 录

序号	姓 名	职 称	单位	论 文 题 目	刊物、会议名称	年、卷、期	类别
1	姚卫星 叶 彬 郑立春	教授 硕士 硕士	011 011 011	A Verification of the Assumption of anti-fatigue Design	International Journal of Fatigue	012301	H
2	金海波 丁运亮	博士 正高	011	Applying object-oriented program technique in the optimum structural design	第四届结构和多学科化国际会议	2001	
3	许志兴 伍华林 丁运亮	博士 正高	011 外校 011	基于信息熵的连续属性自动聚类算法	南京航空航天大学学报	013303	J
4	许志兴 丁运亮 陆金桂	博士 正高 正高	011 011 011	一种基于粗造集理论的粗糙神经网络构造方法	南京航空航天大学学报	013304	J
5	许志兴 丁运亮 熊仲宇	博士 正高 博士	011 011 011	基于退火惩罚混合遗传算法求解生产批量计划问题	南京航空航天大学学报	013301	J
6	熊仲宇 丁运亮 许志兴	博士 正高 博士	011 011 011	利用 Gaussian 型 RBF 网络进行函数逼近的构造性估计	南京航空航天大学学报	013303	J
7	熊仲宇 丁运亮	博士 正高	011 011	确定性的遗传算法	南京航空航天大学学报	013301	J
8	熊仲宇 丁运亮 金海波	博士 正高 博士	011 011 011	Structural Optimization Based on Gas and Hybrid Approximation Technique	第四届结构和多学科优化国际会议	2001	
9	刘芙群 顾仲权	硕士 正高	011 011	智能旋翼-直升机减振降噪的治本技术	国际航空	010008	
10	李春明 汪传生 顾仲权	博士 副高 正高	011 外校 011	非线性结构振动的神经控制	青岛化工学院学报	012201	J
11	李春明 顾仲权 杨卫东	博士 正高 副高	011 011 011	智能旋翼的频域神经控制	航空学报	012205	H
12	袁胜韬 顾仲权	硕士 正高	011 011	旋翼/机身耦合系统的固有特性研究	南京航空航天大学学报	013301	J
13	鲁民月 顾仲权	硕士 正高	011	通用的前馈振动控制 Simulink 仿真系统及其应用	南京航空航天大学学报	013301	J
14	胡宇群	中级	011	Application of response number for dynanic plastic response of plates subjected to impulsive loading	International Journal of Pressure Vessels and Piping	007700	H*
15	胡宇群	中级	011	Scale Effect of Plastic Strain Rate	CHINESE JOURNAL OF AERONAUTICS	011401	H
16	吴海桥 刘 毅 丁运亮	博士 副高 正高	011 011 011	专家系统软件开发生存期模型分析	计算机工程与应用	013720	J

序号	姓　名	职 称	单位	论 文 题 目	刊物、会议名称	年、卷、期	类别
17	吴海桥 刘　毅 丁运亮	博士 副高 正高	011 011 011	大型客机故障诊断初探	航空工程与维修	010004	
18	吴海桥 刘　毅 丁运亮	博士 副高 正高	011 011 011	基于关系数据库的知识库的建立	微型电脑应用	011711	J
19	王适存 徐国华	正高 正高	011 011	直升机旋翼空气动力学的发展	南京航空航天大学学报	013303	J
20	徐国华 王适存 赵景根	正高 正高 硕士	011 011 011	Experimental and analytical investigation on aerodynamics of helicopter scissors tail rotor	Chinese Journal of Aeronautics	011404	H
21	徐国华 王适存	正高 正高	011 011 011	Effects of the shroud on aerodynamic performance in helicopter shrouded tail rotor system	Aircraft Engineering and Aerospace Technology	017306	H
22	徐国华 招启军 高　正	正高 硕士 正高	011 011 011	直升机旋翼对机身气动干扰的计算	第 17 届全国直升机年会	2001	
23	宋彦国 张呈林 徐锦法	博士 正高 博士	011 011 011	Application of fuzzy inference in identification of helicopter model	南京航空航天大学学报（英文版）	011802	J
24	宋彦国 张呈林	博士 正高	011 011	基于自适应模糊系统的直升机悬停/小速度飞行状态下的输出跟踪控制	东南大学学报（自然科学版）	01314A	H
25	于　辉 刘　毅 黄传奇	博士 副高 正高	011 011 011	基于 Web 的民机维护信息管理系统的设计与实现	航空工程与维修	0104202	
26	于　辉 陈　果 左洪福	博士 博士后 正高	011 071 071	内窥技术的发展及在发动机故障诊断中的应用	第四届全国交通领域青年学术会议	2001	
27	张震宇 明　晓	中级 正高	012 012	低速风洞设计中的导流片损失问题	空气动力学学报	011901	J
28	尹江辉 刘　昶	中级 正高	012 012	模糊神经网络在过失速机动飞行中的应用	飞行力学	011901	J
29	周春华	副高	012	创新能力的培养：中西方博士教育之比较	南京航空航天大学学报（社科版）	010302	
30	周春华 唐海敏	副高 本科	012 012	A fictitious domain method for dirichlet problem and its application to generalized stokes problem	南京航空航天大学学报（英文版）	011801	J
31	周春华	副高	012	基于粘接元技术的区域分裂解法及其应用	空气动力学学报	011901	J
32	陆志良	正高	012	Generation of dynamic brids and couputation of unsteady transonic flowsround asseurbles	Chinese Journal of Aeronautics	011401	H
33	张　强 王华明 胡章伟	副高 副高 正高	012 012 012	直升机噪声信号的小波分析	声学学报	012605	H
34	黄　达 李志强 吴根兴	副高 中级 正高	012 012 012	飞机平尾偏转对大迎角动态气动特性的影响	航空学报	012203	H
35	刘学强 伍贻兆 夏　健	中级 正高 中级	012 012 012	混合网格在求解三维 N-S 方程中之应用	南京航空航天大学学报	013304	J

序号	姓　名	职 称	单位	论 文 题 目	刊物、会议名称	年、卷、期	类别
36	刘学强 伍贻兆	中级 正高	012 012	非结构网格 N-S 方程解法研究及在多段翼型绕流中之应用	空气动力学学报	011902	J
37	王江峰 伍贻兆	中级 正高	012 012	三维横向喷流与超音速主流干扰流场之数值模拟	宇航学报	012206	H
38	王江峰 伍贻兆	中级 正高	012 012	基于基因算法与博奕论的翼型跨音速 Euler 方程气动优化	南京航空航天大学学报	013306	J
39	吕宏强 伍贻兆 夏　健	博士 正高 中级	012 012 012	非结构多重网格流场数值模拟研究	空气动力学学报	011904	J
40	夏　健	中级	012	Truncation error reduction method for planar cavity flow	南京航空航天大学学报（英文版）	011802	J
41	伍贻兆 刘学强 夏　健	正高 中级 中级	012 012 012	The solution of 3D turbulence naner-stokes equations using mpoid grids	“连续物理的计算与应用”国际会议	2001	
42	伍贻兆 张　辉	正高 正高	012 机关	我国经济体制转型期高校产学研合作教育新情况及应对策略	南京航空航天大学学报（社会科学版）	010301	
43	夏　浩 唐登斌 陆昌根	硕士 正高	012 012 012	边界层流动的非平行稳定性研究	空气动力学学报	011902	J
44	唐登斌	正高	012	大小鱼相从，排云结队行	力学与实践	012305	H
45	唐登斌 王伟志 梁红光	正高 博士 硕士	012 012 012	大雷诺数翼型非定常运动问题研究	固体力学学报	012205	H
46	姚　裕 姚学升 吴洪涛	硕士 硕士 正高	012 051 051	模块化 6-SPS Stewart 机床位置参数识别	华东船舶工业学院学报	011501	J
47	黄明恪	正高	012	任意二维物体捕捉自由涡的驻定态稳定性分析	空气动力学学报	011903	J
48	胡文蓉 黄明恪	硕士 正高	012 012	三角形突起物后自由旋涡的稳定性	流体力学实验与测量	011501	J
49	唐智礼 黄明恪	博士后 正高	012 012	基于控制理论的 Euler 方程翼型减阻优化设计	空气动力学学报	011903	J
50	隋洪涛 陈红全 黄明恪	博士 正高	012 012 012	基于 Euler 方程的翼型优化设计高效基因算法研究	南京航空航天大学学报	013304	J
51	沈宏良 刘　昶	中级 正高	012 012	飞机平衡状态的优化计算方法	飞行力学	011904	J
52	沈宏良	中级	012	遗传算法在试飞科目最优排序问题中的应用	飞行力学	011901	J

此为试读，需要完整PDF请访问：www.ertongbook.com

ELSEVIER

International Journal of Fatigue 23 (2001) 271–277

International Journal of Fatigue

www.elsevier.com/locate/ijfatigue

Technical note

A verification of the assumption of anti-fatigue design

Weixing Yao *, Bin Ye, Lichun Zheng

Department of Aircraft Engineering, Nanjing University of Aeronautics and Astronautics, Nanjing 210016, PR China

Received 1 March 2000; received in revised form 29 July 2000; accepted 4 September 2000

Abstract

In this paper, the approaches of anti-fatigue design are briefly reviewed and are classified into three groups: nominal stress approach, local stress–strain approach and stress field intensity approach. Two types, each with two notches, are specially designed and a total of 30 specimens with 4 dimensions are tested under different constant–amplitude loading. These specimens are also analysed with elasto-plastic FEM to obtain stress–strain distributions and stress concentration factors. Fatigue life is estimated based on the different approaches. Experimental and analytical results show that the assumption of stress field intensity is more reasonable than that of the other approaches. © 2001 Elsevier Science Ltd. All rights reserved.

Keywords: Design against fatigue; Nominal stress approach; Local stress–strain approach; Stress field intensity approach; Fatigue experiment

1. Introduction

Metal fatigue is a complicated phenomenon which depends on many factors, and up to now the description of fatigue crack initiation has been left for further investigation. Notches in engineering structures are always the critical places for fatigue failures, so the prediction of fatigue life or fatigue strength of notched elements is the key point of the structure design against fatigue. In the history of fatigue research, many approaches [1,2] for the prediction of fatigue life of notched elements have been developed. Most of the approaches can been classified into three types according to their assumptions: nominal stress approach (NSA), local stress–strain approach (LSSA) and stress field intensity approach (SFIA). In this paper two types of specimens, each with two notches, are designed and tested under different constant–amplitude loading to see which assumption of the approaches is the most reasonable.

2. A brief review of the approaches

The approaches for prediction of fatigue life have been reviewed in detail in some of the literature [1–3]. Most of the approaches can be classified into the following three groups: NSA, LSSA and SFIA.

2.1. Nominal stress approach (NSA)

The assumption of the NSA is that the fatigue life of elements with different notches is the same if these notches have the same theoretical stress concentration factors and are under the same loading history (Fig. 1).

Obviously the nominal stress S and theoretical stress concentration factor K_T are the control parameters in this approach. But in practice, the fatigue life predicted by this approach is far removed from the fatigue life obtained by fatigue experiments in most cases. Many

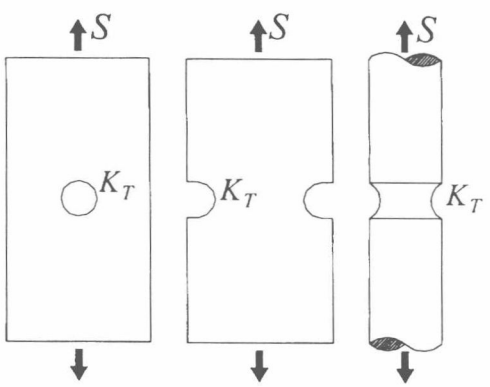

Fig. 1. Nominal stress approach.

* Corresponding author. Tel.: +86-25-489-2177; fax: +86-25-489-1422.

E-mail address: wxyao@nuaa.edu.cn (W.X. Yao).

0142-1123/01/$ - see front matter © 2001 Elsevier Science Ltd. All rights reserved.
PII: S0142-1123(00)00083-9

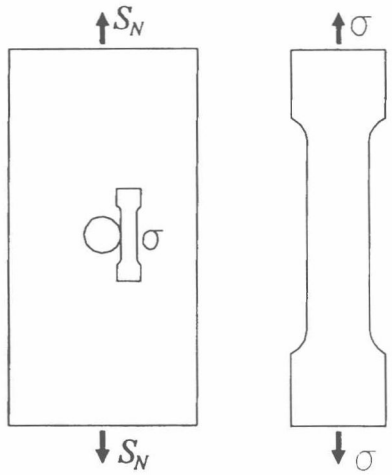

Fig. 2. Local stress–strain approach.

other models, such as the stress severity factor (SSF), effective stress method, and detailed fatigue rating (DFR), belong to this approach [1].

2.2. Local stress–strain approach (LSSA)

The assumption of the LSSA is that the fatigue life of elements with different notches is the same if the local stress–strain histories at the roots of the notches are the same (Fig. 2).

The LSSA is a point criterion. The local stress and local strain are the control parameters of fatigue life of notched elements [4]. Many kinds of LSSA have been formed with the combination of the cyclic stress–strain relationship of the material, the strain–life curve of the material, the fatigue damage cumulative rule and the solution of the local stress–strain at the notch.

In practice, the fatigue life estimated based on the real local stress and strain is lower than the fatigue life obtained by the fatigue test, so usually the fatigue notch factor K_f is used to calculate the local stress and strain in Neuber's equation instead of theoretical stress concentration factor K_T. Many researchers [5] have made efforts to estimate the K_f accurately, and Peterson's equation is the most popular method [6].

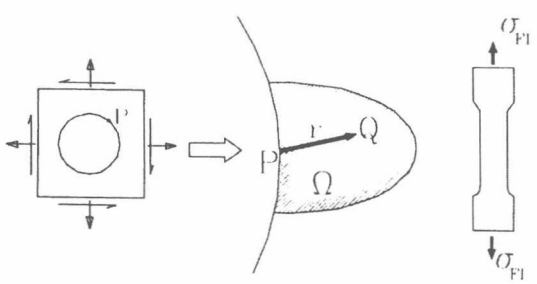

Fig. 3. Stress field intensity approach.

2.3. Stress field intensity approach (SFIA)

The assumption of the SFIA is that the fatigue life of the elements with different notches is the same if the stress field intensity histories are the same (Fig. 3) [7–9].

SFIA defines the stress field intensity σ_{FI} as:

$$\sigma_{FI}=\frac{1}{V}\int_{\Omega} f(\sigma_{ij})\varphi(\vec{r})\mathrm{d}v \tag{1}$$

where Ω is the fatigue failure region and V is the volume of Ω which only depends on the material, $f(\sigma_{ij})$ is the failure function and $\varphi(\vec{r})$ is the weight function. A brief discussion of Eq. (1) follows.

2.3.1. The fatigue failure region Ω

From the point of view of the fatigue mechanism, crack initiation generally occurs within the local region near the surface of the specimen where stress increases. This region is several grain sizes in extent. So the size and form of Ω depend on the material.

2.3.2. The failure function $f(\sigma_{ij})$

$f(\sigma_{ij})$ is the function to describe crack initiation under multiaxial stress, and may be different for different materials. For example, Von Mises' equivalent stress is used for elasto-plastic materials, such as carbon steel, aluminum alloy and titanium, and maximum major stress is used for materials such as cast iron and cast steel. $f(\sigma_{ij})$ contains the effect of multiaxial stress near a notch, so the SFIA can deal with fatigue strength under multiaxial loading.

2.3.3. The weight function $\varphi(\vec{r})$

The weight function $\varphi(\vec{r})$ physically means the contribution of stress at Q to the peak stress at $|\vec{r}|=0$.

1. $0\leq\varphi(\vec{r})\leq 1$ *and* $\varphi(\vec{r})$ *is a generalised monotonically* decreasing function about $|\vec{r}|$;
2. $\varphi(0)\equiv 1$ which means that the contribution of the stress at the notch root is maximum;
3. when the stress gradient $G=0$, $\varphi(\vec{r})\equiv 1$, which is consistent with the condition of smooth specimens.

$\varphi(\vec{r})$ is not only related to notch geometry and loading type for isotropic materials, but also to material properties for anisotropic materials. It can be obtained analytically or numerically and as an approximation of first order the following expression is used in this paper:

$$\varphi(\vec{r})=1-cr(1+\sin\theta) \tag{2}$$

where c is a factor related to stress gradient.

Table 1
A brief comparison among the three approaches

	Failure place		
	Stress concentration NSA	Notch root LSSA	Local region near notch SFIA
Control parameters	K_T and nominal stress K_TS	Local stress and local strain $K_\rho S$ and σ_{max}	Stress field intensity σ_{FI}
Material properties	S–N curves under different K_T and R	Cyclic σ–ε relationship ε–N_f curve (K_T=1)	Cyclic σ–ε relationship S–N or ε–N_f curve under K_T=1

Table 2
The chemical and mechanical properties of aluminum alloy LY12-CZ

(a) Chemical properties of aluminum alloy LY12-CZ

Elements	Cu	Mg	Mn	Fe	Si	Zn	Ni
Wt%	4.61	1.54	0.58	0.29	0.26	0.10	0.024

(b) Mechanical properties of aluminum alloy LY12-CZ

Young's Modulus E (MPa)	Ultimate strength σ_b (MPa)	Yield strength σ_Y (MPa)
71022	466	343

2.3.4. The failure criterion

For a smooth specimen, K_T=1, G=0 and then $\varphi(\vec{r})$=1. The stresses in the smooth specimen are equal everywhere, i.e. $f(\sigma_{ij})\equiv constant$. According to Eq. (1), $\sigma_{FI}=f(\sigma_{ij})$. Obviously, when $\sigma_{FI}=f(\sigma_{ij})\geq\sigma_f$, fatigue failure occurs for a smooth specimen. Because Eq. (1) is universally applicable to notched specimens as well as to smooth ones, the failure criterion can be written as:

$$\sigma_{FI}\geq\sigma_f \tag{3}$$

2.4. A brief comparison among the three approaches

From the above discussion it can been seen that the assumptions of the three approaches are different, and the material properties required for each approach are also different. Table 1 gives a brief comparison of the three approaches.

3. Experiments

3.1. Specimens

Two types of specimens are specially designed and tested under different constant-amplitude loadings to verify the assumptions of the approaches.

Specimens are made from aluminum alloy LY12-CZ plate with thickness of 2 mm. The chemical and mechanical properties are listed in Table 2. They are cut longi-

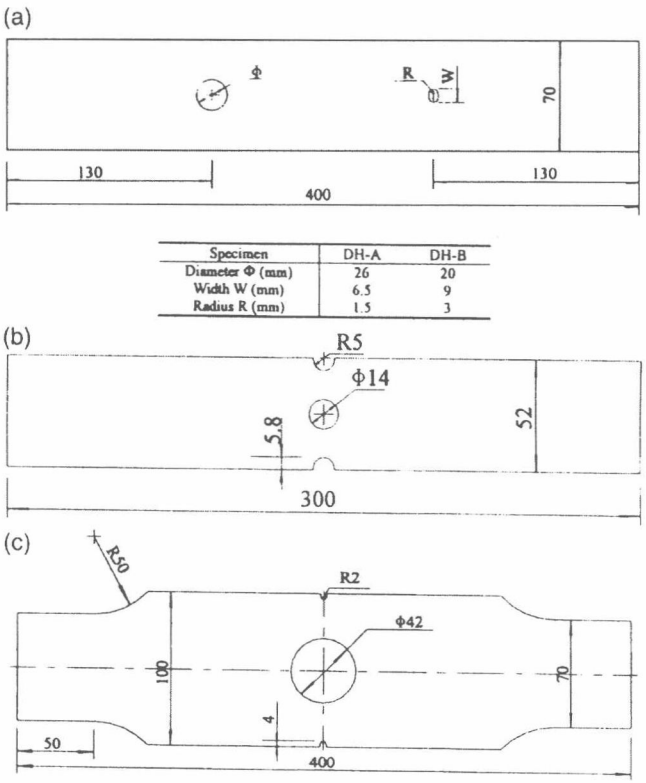

Fig. 4. (a) Double-hole specimen (DH). (b) Double-notch specimen (DN-A). (c) Double-notch specimen (DN-B).

Table 3
Experimental results of the double-hole specimens

Specimen	Loading (MPa)	Frequency (Hz)	Fatigue life	The place where the crack initiated
DH-A01	80	12	122 734	One side of the hole
DH-A02	80	12	113 000	One side of the hole
DH-A03	80	12	169 235	One side of the hole
DH-A04	80	12	144 708	One side of the hole
DH-A05	80	12	122 469	One side of the hole
DH-A06	80	12	143 164	One side of the hole
DH-A07	150	6	15 900	One side of the hole
DH-A08	150	6	18 952	One side of the hole
DH-A09	150	6	18 518	Both the side of the hole
DH-A10	150	6	16 426	One side of the slot
DH-A11	150	6	15 649	One side of the hole and one side of the slot
DH-A12	150	6	17 741	Both the side of the hole
DH-B01	98	14	136 600	One side of the slot
DH-B02	98	14	181 890	One side of the slot
DH-B03	98	14	166 300	One side of the slot

Table 4
Experimental result of the double-notch specimens

Specimen	Loading (MPa)	Frequency (Hz)	Cycles to failure	The places where cracks initiate
DN-A01	78.4	20	335 530	One edge notch
DN-A02	78.4	22	143 440	One edge notch
DN-A03	78.4	22	192 950	One edge notch
DN-B01	80	8	73 320	One side of the hole
DN-B02	80	8	74 962	One side of the hole
DN-B03	80	8	76 178	Both the sides of the hole
DN-B04	80	8	67 342	One side of the hole and one notch
DN-B05	80	8	74 694	One side of the hole
DN-B06	80	8	90 205	Both the sides of the hole
DN-B07	100	6	33 241	One side of the hole
DN-B08	100	6	33 919	One side of the hole
DN-B09	100	6	26 285	Both the sides of the hole
DN-B10	100	6	47 784	One side of the hole
DN-B11	100	6	19 336	Both the sides of the hole
DN-B12	100	6	25 500	One side of the hole

Table 5
Cyclic stress–strain curve of aluminium alloy LY12-CZ

Stress (MPa)	Strain	Stress (MPa)	Strain
0	0	371	0.01300
249	0.00356	382	0.01800
309	0.00450	396	0.02500
327	0.00500	415	0.04000
337	0.00550	451	0.08000
348	0.00700	462	0.10000
355	0.00850	466	0.11500
361	0.01000	470	0.01510

tudinally from the same plate to diminish scatter. A double-hole specimen has two separate notches, one is a hole and the other is a slot [Fig. 4(a)]. A double-notch specimen has three separate notches, one is a central hole and the others are edged notches [Fig. 4(b) and (c)].

3.2. Experiment

The experiment is carried out at the MTS 810. For the 12 DH-A specimens, 6 specimens are tested under a nominal stress of 80 MPa, other specimens under 150 MPa, and 3 DH-B specimens are tested under 98 MPa. The experimental results are listed in Table 3. Three specimens labelled DN-A are tested under a constant–

Table 6
Analytical results of the specimens (stress: MPa)

Specimen	K_T (gross)	K_T (net)	K_f[a]	Loading S	σ_{max}	σ_{FI}
The hole of specimen DH-A	3.61	2.27	2.19	80	286.11	247.62
				150	363.55	320.06
The slot of specimen DH-A	3.96	3.42	2.68	80	297.66	239.33
				150	366.55	319.24
The hole of DH-B	3.42	2.44	2.34	98	316.64	276.06
The slot of DH-B	3.50	2.75	2.43	98	341.40	279.23
Hole of DN-A	1.64	1.64	1.51	78.4	253.47	224.12
Edge-notch of DN-A	1.74	1.74	1.57	78.4	266.53	230.10
Hole of DN-B	2.04	2.04	1.99	80	303.91	261.89
				100	378.86	298.93
Edge-notch of DN-B	2.08	2.08	1.71	80	309.31	250.45
				100	386.65	292.40

[a] K_f is calculated based on Peterson's equation, and the constant α_0=0.63 [11].

Table 7
Estimated and experimental fatigue life

Failure place		LSSA (Neuber)	NSA	SFIA	Experiment (average)
The hole of DH-A	S=80 MPa	42 053	706 891	202 770	135 885
	S=150 MPa	1963	46 212	32 773	17 352
The slot of DH-B	S=98 MPa	46 509	780 981	96 746	161 597
Edge-notch of DN-A	S=78.4 MPa	78 487	495 669	295 802	223 973
Hole of DN-B	S=80 MPa	33 302	329 583	146 617	76 117
	S=100 MPa	11 926	124 903	58 487	31 011

amplitude loading of 78.4 MPa. For the 12 specimens labelled DN-B, 6 specimens are tested under a nominal stress of 80 MPa, and the other specimens under 100 MPa. The experimental results are listed in Table 4. The fatigue life listed in the Tables 3 and 4 is the number of cycles to a crack size of about 0.5 mm, which is determined by microscopic monitoring during the experiment, and fractography after the experiment.

3.3. Analysis

NASTRAN was employed for elasto-plastic FE analysis to calculate the stress–strain distribution and stress field intensity σ_{FI} of the specimens. The cyclic stress–strain curve, which is listed in Table 5, is used in the elasto-plastic FE analysis. The analytical results are listed in Table 6. Von Mises effective stress is taken as the fatigue failure function $f(\sigma_{ij})$ and the size of the fatigue failure region for LY12-CZ aluminum is 0.185 mm [10] in calculating SFI σ_{FI} with Eq. (1).

Fig. 5 presents Von Mises stress distribution along the line at the minimum width of the double-hole specimens. It can be seen that the maximum stress is at the edge of the slot, but the stress decreases faster, so the stress field intensity of the hole is larger than that of the slot. Fig. 6 presents Von Mises stress distribution along the line at the minimum width of the double-notch specimens. The maximum stress occurs at the edged notches, but the stress decreases faster, which means that the stress field intensity of the central hole is larger.

Table 7 presents the fatigue life predicted by the different approaches. Miner's rule is used in the prediction. The S–N curve for the NSA is listed in Table 8 and the strain–life curve $\varepsilon-N_f$ for LSSA is expressed by Eq. (4).

$$\log N_f = A_0 + A_1 \tan h^{-1}\left\{\frac{\log(\varepsilon_u \varepsilon_e/\varepsilon_{eq}^2)}{\log(\varepsilon_u/\varepsilon_e)}\right\} \tag{4}$$

where effective strain $\varepsilon_{eq}=(2\varepsilon_a)^m\left(\frac{\sigma_{max}}{E}\right)^{1-m}$, σ_{max} is maximum local stress, m=0.4, A_0=3.4328, A_1=2.7551, ε_u=0.053, and ε_e=0.0135 are material constants.

4. Discussion

Comparing the analytical results with the experimental results, it can be seen that stress gradient is a very important parameter for the prediction of fatigue life, as well as the peak stress. In fact this argument had been put forward several decades earlier [12] and many models developed to find a way to take into consideration the two factors properly. The SFIA is one new such model which gives a parameter σ_{FI} as the intensity of

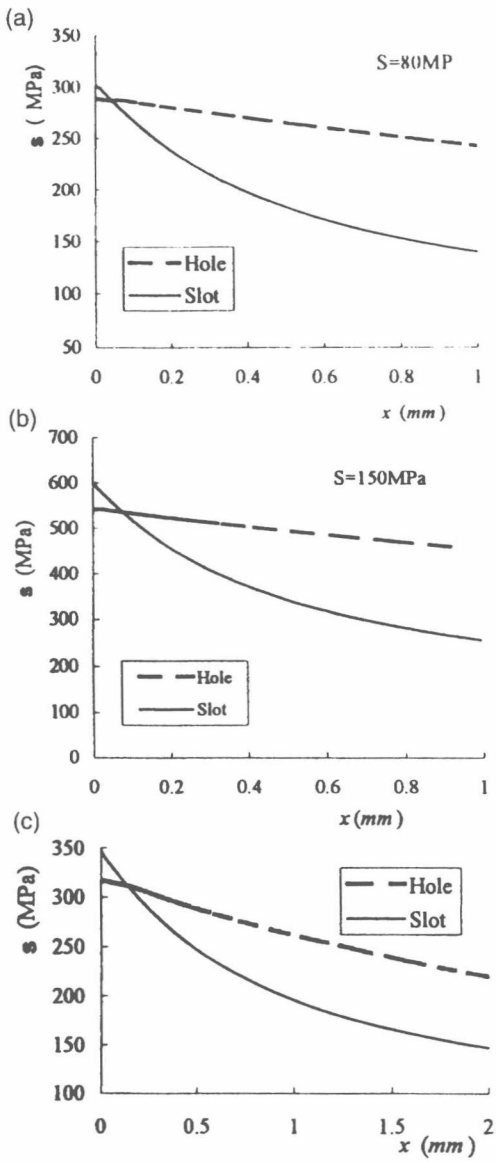

Fig. 5. (a) The stress distribution at the minimum width of the specimen DH-A (S=80 MPa). (b) The stress distribution at the minimum width of the specimen DH-A (S=150 MPa). (c) The stress distribution at the minimum width of the specimen DH-B (S=98 MPa).

the stress field near the notch. For the double-hole specimens DH-A and DH-B, the maximum stress at the roots of the slots is larger than that at the roots of the holes (Table 6), but the fatigue crack initiated at the root of the hole (Table 3). For the double-notch specimens DN-A and DN-B, the same conclusion can be obtained from Tables 4 and 6.

For specimen DH-A, the SFI of the hole is nearly the same as that of the slot under load S=150 MPa, which means that the fatigue cracks initiated at the slot of two specimens and at the hole of five specimens. Among them, fatigue cracks initiated at both the hole and the slot almost simultaneously for specimen DH-A11.

The fatigue life predicted by the SFIA is closest to

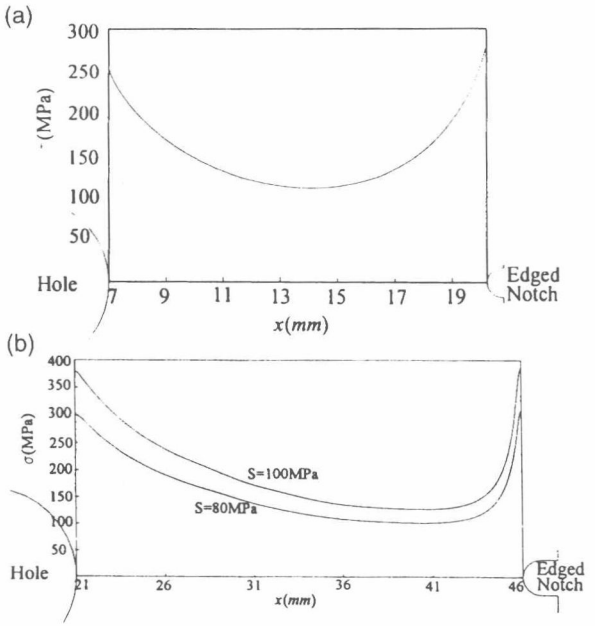

Fig. 6. (a) The stress distribution at the minimum width of the specimen DN-A. (b) The stress distribution at the minimum width of the specimen DN-B.

Table 8
S–N curve of aluminum alloy LY12-CZ (R=0.1)

Stress S (MPa)	Cycles to failure N
400	2560
350	19 100
300	83 976
250	311 050
200	572 296
180	600 260
170	846 313
160	1 309 410

the experimental results on the average because the S–N curve and the cyclic stress–strain curve are with 50% survival. The prediction of fatigue life by the LSSA is good for low-cycle fatigue, and prediction by the NSA is much more conservative.

5. Conclusions

The following conclusions can be drawn according to the above experiments and analysis.

1. The maximum stress at the root of the notch is not the control parameter of fatigue crack initiation, because the stress gradient plays a very important role.
2. Stress field intensity σ_{FI} is the control parameter of fatigue crack initiation since the peak stress and the

此为试读,需要完整PDF请访问: www.ertongbook.com

stress gradient are properly considered in this approach.

3. $K_T S$ is not the control parameter of fatigue crack initiation.
4. The fatigue life predicted by the SFIA is more accurate than the other approaches.

References

[1] Zheng LC, Yao WX. A review of approaches for predicting fatigue crack life. Mechanics and Practice 1996;18(4):9–15 [in Chinese].

[2] Duggan TV, Byrne J. Fatigue as a design criterion. Macmillan Press Ltd, 1977.

[3] Suresh S. Fatigue of materials. Cambridge, 1998.

[4] Dowling NE, Brose WR, Wilson WK. Notched member fatigue life prediction by the local stress strain approach. In: Wetezl RM, editor. Fatigue under complex loading — analysis and experiments., 1977:55–84.

[5] Yao WX, Xia KQ, Gu Y. On the fatigue notch factor K_f. Int J Fatigue 1995;17(4):245–51.

[6] Peterson RE. Notch sensitivity. In: Sines G, editor. Metal fatigue. McGraw-Hill, 1959:293–306.

[7] Yao WX. Stress field intensity approach for prediction of fatigue life. Int J Fatigue 1993;15(3):243–5.

[8] Yao WX. On the notched strength of composite laminates. Composite Sci Technol 1992;45:105–10.

[9] Yao WX. The prediction of fatigue behaviour by stress field intensity approach. Acta Mech Sol Sin 1996;9(4):337–49.

[10] Zheng LC. Research on the fatigue life of crack initiation based on stress field intensity approach, Master Thesis. P.R. China: Nanjing University of Aeronautics and Astronautics; 1996.

[11] Neuber H. Theory of stress concentration for shear strained prismatical bodies with arbitrary nonlinear stress–strain law. J Appl Mech ASME 1961;28(4):544–50.

[12] Jhansale HR. A unified approach for modeling inelastic behaviour of structural metals under complex cyclic loadings. AD-A040741, 1977.

第四届结构和多学科优化国际会议
2001.6.4. — 6.8. 中国、大连

Applying object-oriented program technique in the optimum structural design

Jin Haibo **Ding Yunliang**

(School of Aeronautics and Astronautics, Nanjing University of Aeronautics and Astronautics, Nanjing 210016)

1. Abstract

OOP (Object-oriented program) can be used to improve the structural optimization design and FEA (finite element analysis) programs. This paper describes the problem associated with conventional software and the potential solutions offered by OOP.

The first is applying OOP to encapsulate the FEM (finite element model) data. This encapsulation would increase FEA software extendibility and flexibility, needed in studying new FEA method and design of structural optimization program. The second is applying OOP to encapsulate FEA, sensitivity analysis and optimization solution methods, which once are couple with the FEM data. So efficiently encapsulation on these solution methods would simplify the study of the FEA and optimization solution methods. The third is applying OOP to unify the size optimization and shape optimization in a uniform mode, which would simplify the solution of their couple problem while using in a synthesis mode in conventional optimization problem.

2. Keywords: structural optimization design, object-oriented program, finite element analysis

3. Introduction

Conventional structural optimization design program, which is consisted of several dozens of subroutines and functions, are programmed by the method from top to down and stepwise. These dozens of subroutines and functions complex the global data structure, and decrease the flexibility of the system. It is difficult to modify the existing codes and extend the code to adapt them for new use. The application of OOP has proven to be very beneficial to development of flexible programs. The basis of OOP is abstraction, whose philosophy abstract out the essential immutable qualities and procedures of the components of the structural optimization design into classes of objects. Objects store both their data and the operators on the data that may be used by other objects. The abstraction of the data into classes of objects limits the knowledge of the system required to work on the code, to only the class of interest. Encapsulation on the data and operations together isolates the classes and promotes the reuse of code. This paper demonstrates a new object-oriented architecture for structural optimization design. The goal of the system is to provide a flexible and extendible set of objects that facilitate optimization. The flexibility is achieved by the separation of the optimization tasks into distinct objects. The primary separation isolates the numerical objects and algorithms of the structural optimization design as well as FEM data into distinct two types of object classes.

4. Finite element model object classes

FEM are the basis of structure optimization design. Conventional structure optimization's algorithms rely on the efficient manage FEM information, especially on the shape optimization and the topology optimization of the structure. Conventional FEM consist of nodes, elements, materials, boundary conditions and loads, whose attribute data are interdependent on each other. If these data are accessioned from the global variables, they would decrease the flexibility of the system. FEM object classes abstract from the conventional FEM into six distinct base objects, which further derive into all kinds of FEM object classes. The six base object classes are node object classes, element object classes, property object classes, material object classes, boundary condition object classes and load object classes. Because these object classes are interdependent and couple, we need build a top object class, the FEM manage object class, which manages blending the communication of the six distinct classes and transferring the information between the FEM and the solutions of the FEA and the optimization.

5. Analysis and optimization solution object classes

Typical optimization tasks include finite element analysis, sensitivity analysis and optimization solution method. Later, it will demonstrate how to apply OOP to encapsulate these tasks.

5.1 Finite element analysis

The typical finite element analysis equation is expressed as:

$$[k]\{u\} = \{p\}. \tag{1}$$

Distinct from normal linear equations, the matrix $[k]$ in the equation (1) is a large sparse matrix. We don't store all members of the matrix in the two dimensional array, but in a unified contract array. We need build a matrix object class, which map the global large sparse stiffness matrix and local small stiffness matrix. So we abstract equation (1) into the stiffness matrix and the displacement vector object classes as well as an independent module, which is used to solve the specific linear stiffness matrix equations. The two object classes contain the FEM manage object class' handle, which can transfer the FEM attribute values into the stiffness matrix object class and node displacement object class. The independent module has contained these two object classes, which support the solution method is independent to FEM. The solution procedure gets FEM information only through these two object classes. The module's head declaration can be expressed as:

```
BOOL Matrix_Solve(CStiffMatrix* matrix, CDisplacement* disp, BOOL decompose );
```

5.2 Sensitivity analysis

Sensitivity analysis's important step is to solve the derivatives of the displacement to the design variables. Its equation is expressed as:

$$[k]\left\{\frac{\partial u}{\partial t_j}\right\} = \{q\}. \tag{2}$$

Equation (1) and equation (2) have the same type and the same stiffness matrix $[k]$, so we derive the sensitivity analysis object class from the FEA object class. The derivation makes the sensitivity analysis object class inherit the FEA object class's member functions and solution methods. Distinct from the FEA, the sensitivity analysis needs to solve the derivation of related element stiffness matrix to the design variables. So the sensitivity analysis object class encapsulates the computation procedure of the derivation of element stiffness matrix. The computation derivation is related with the design variables, which is introduced later. The design variable object directs the sensitivity analysis to adjust some FEM attribute value and the sensitivity analysis object encapsulates the derivation solution method.

5.3 Optimization solution method

Typical optimization expression can be:

$$\begin{aligned} &\min.\ w(X) \\ &s.t.\quad g_i(X) \le g_i \quad i = 1,2,\cdots,m,\ \text{m is the number of constraints} \\ &\qquad x_j^L \le x_j \le x_j^U \quad j = 1,2,\cdots n,\ \text{n is the number of design variables} \end{aligned} \tag{3}$$

Before we abstraction the equation (3), we need to build a design variable object class. Abstracted from all kinds of application, the design variable object class provides the uniform expression for the variable adjustment by the polymorphism of OOP technique. Then we abstract the equation (3) into an optimization object class, in which we utilize the polymorphism of OOP technique to uniformly encapsulate the solution of the object functions and constraint functions. So any specific optimization problem can derive from the optimization object class into a specific optimization object class, whose solution of object function and constraint functions will be rebuilt based on the specific optimization problem. The optimization object class also containes an array of design variable object classes and an independent module, which is solving the optimization problem. The typical optimization solving module's head declaration can be expressed as:

BOOL Optimization_Solve (COptimization* opt);

As the support of the optimization base object class, the optimization solution module can be independent to any specific optimization problem and has no relationship with the solution of object function and constraint functions, which is analogous to the subroutine's function parameter in the FORTRAN.

6. Size optimization and shape optimization

Size optimization and shape optimization have different types of design variables. In the conventional structural optimization design, they are implemented by different subroutines and functions. Now, applying OOP technique can blend the two types optimizations in the same optimization procedure. We derive from normal optimization object class into specific structural optimization design object class, which containes the size and shape algorithm operators object classes in the same uniform. Derived from the design variable object class, the size operator and shape operator object classes encapsulate the design variable operation method and the method how design variable is linked to FEM attribute value. The size operator object class is linked to the elements' internal attribute value and the shape operator object class is linked to the nodes' position attribute or the control points which are control nodes position. These encapsulated operators also contain adjustment of value of the design variables and judgment on the design variables out of the feasible domain range.

7. Conclusion

An object-oriented structure optimization program has proven that the program is flexible, extendible, easily modified for a variety of structure optimization design procedures. The problems inherent in procedural based optimization programs are eliminated by design. To modify or extend the program, the required knowledge of the components is restricted to the public interfaces of the classes. The reuse of code is promoted by the use of inheritance.

8. References:

[1] Forde BWR, Faschi RO & Stiemer SF, Object-oriented finite element analysis, Computers and Structures, 1990, 34:355-74.

[2] Miller GR, Coordinate-free isoparametric elements, Computers and Structures, 1993, 49:1027-35.

[3] Archer GC, Fenves G & Thewalt C, A new object-oriented finite element analysis program architecture, Computers and Structures, 1999, 70: 63-75.

[4] Yanez, D.P., Hauch, R.M., Prey & S.W., A Rapid Method For Creating High Fidelity Finite Element Models, AIAA-99-1301.

[5] Jing-Sheng Liu, geoff Parks & John Clarkson, Metamorphic development: A new topology optimization method for truss structures, AIAAA-99-1387.

[6] Ding Yunliang, Applied optimum design of engineering structures, Nanjing University of Aeronautics and Astronautics Press, 1990.7

第 33 卷第 3 期
2001 年 6 月

南京航空航天大学学报
Journal of Nanjing University of Aeronautics & Astronautics

Vol. 33 No. 3
Jun. 2001

文章编号:1005-2615(2001)03-0233-04

基于信息熵的连续属性自动聚类算法

许志兴[1)]　伍华林[2)]　丁运亮[1)]

([1)]南京航空航天大学航空宇航学院　南京,210016)

([2)]华东电子集团公司　南京,210028)

摘要　基于信息熵的有关理论,提出了一种新的连续属性的自动聚类算法。首先介绍了 Shannon 熵的概念及其两个重要的定理,基于信息的不确定测度,提出了一种 Shannon 熵的准则函数 φ,并且指出了该准则函数必须满足的 6 条原则。其次,基于该准则函数,引出了一种针对单个连续属性自动聚类的 FUSINTER 算法。由于实际信息系统中有多个连续属性,这就需要对多个连续属性分别使用 FUSINTER 算法进行离散,并且要求最终保证整个信息系统离散后是相容的和一致的,而且各个属性拥有较少的分割区间。最后,本文以干线飞机外形参数的变化趋势与其更新换代的关系来说明文中提出的连续属性离散化过程,并展示了该聚类算法的有效性。本文提出的方法可以用于机器学习或数据挖掘的数据前处理。

关键词:熵;聚类;连续属性;类别属性;离散化;FUSINTER 算法

中图分类号:TP18　　**文献标识码**:A

引　言

数据挖掘是当今国际人工智能和数据库研究的最活跃的新兴领域之一,是数据库中知识发现 KDD(Knowledge discovery in databases)的核心,它为大量数据的利用提供了有效的工具。数据库中聚类的对象是例子(记录或元组),每个例子由不同的属性构成,这些属性分为两大类:布尔型属性和多值属性,而多值属性又分为连续属性(又称数量属性)和类别属性。在机器学习或数据挖掘中,连续属性的处理比较复杂,一般方法是把它转化为类别属性或布尔属性,这样问题就在于如何把数据聚类或映射为类别属性或布尔属性。

聚类的目标是将数据聚集成类,使得类间的相似性尽量小,类内的相似性尽量大。分类问题(有监督)和聚类问题的根本不同点在于:分类问题中,知道训练样本的分类属性值,而在聚类问题中,就需要在训练样本中找出这个分类属性值。目前流行的聚类算法一般分为概念分层聚类和数据分割聚类。概念分层聚类也称概念提升或概念泛化,就是利用属性的概念树进行概念爬升的过程,使属性的一个较具体的值被概念树上的父概念替代,并对基表中的相同元组进行归并,计算归并后得到宏元组所覆盖的元组数。通过概念提升,使得属性域取值的抽象程度提高,从而完成归纳过程。数据分割聚类是通过优化一个评价函数把数据集分割为一些区间,从而达到聚类的目的。

作为一种知识表示结构,聚类可由知识工程师、领域专家或用户提供。但对于大型数据库,属性繁多,数据量极大,使用人工知识或经验对属性值进行聚类显然是不现实、不合理的。另外,对于特殊的数据挖掘任务要求构造专门的概念层次,反映特殊数据集合中的数据分布。因而对连续属性值进行自动聚类,满足大型数据库中的特殊挖掘任务的要求,是当前数据挖掘面临的迫切任务。许多学者已经做了大量的工作。Kerber[1]提出的 ChiMerge 算法、Fayyad[2]提出的 MDLPC 算法以及 Zighed[3]提出的 FUSINTER 算法可将连续属性离散化。Han 和 Fu[4]研究了数据挖掘任务中数值型概念层次的

收稿日期:2000-06-20;**修订日期**:2000-10-20

作者简介:许志兴,男,博士研究生,1970 年 6 月生;伍华林,男,工程师,1966 年 10 月生;丁运亮,男,教授,博士生导师,1941 年 1 月生。

自动生成和动态调整，提供了相应的算法，并把它应用于面向属性的归约技术。Cheung[5]提出了基于规则的概念层次。蒋嵘[6]通过云变换实现了泛概念树的自动生成。

本文介绍了信息熵的概念，研究了基于信息熵的连续属性值聚类的自动生成算法。

1 基于信息熵的概念表示

定义 1[7] 设 X 是取有限个值的随机变量，$p_i=P\{X=x_i\}$，$i=1,2,\cdots,n$，则 X 的熵定义为

$$H(X)\triangleq\sum_{i=0}^{n}p_i\log_a\frac{1}{p_i}$$

其中，对数的底 a 可为任何正数，一般取 2，规定当 $p_i=0$ 时，$p_i\log_a\frac{1}{p_i}=0$。

上面定义的熵，一般称为 Shannon 熵，它是美国工程师 C. E. Shannon 在 1948 年首先提出来的，后来人们几次改进，但一直没有大的变化，所以一直沿用至今。但是 Shannon 熵实质上只适用于有限场的情况，连续型随机变量的场合根本不适用。因此对连续属性必须先离散化，才能够使用 Shannon 熵进行信息处理。

Shannon 熵有两个重要的定理[7]，即：

定理 1 $H(p_1,p_2,\cdots,p_n)\geqslant 0$，其中等号成立当且仅当对某 i，$p_i=1$，其余的 $p_k=0(k\neq i)$。这表明确定场（无随机性）的熵最小。

定理 2 $H(p_1,p_2,\cdots,p_n)\leqslant\log_2 n$，其中等号成立当且仅当 $p_k=\frac{1}{n}$，$k=1,2,\cdots,n$。这表明等概场具有最大熵。

设 X 为任一连续条件属性，将它划分成 k 个区间 $I_1,I_2,\cdots,I_k$，设决策属性 d 存在 m 个分类，则有：

n_{ij}：区间中属于分类的样本数目；

n_j：区间中的样本数目，有 $n_j=\sum_{i=1}^{m}n_{ij}$；

n_i：属于分类的样本数目，有 $n_i=\sum_{j=1}^{k}n_{ij}$；

n：样本数目，有 $n=\sum_{j=1}^{k}n_j$ 或 $n=\sum_{i=1}^{m}n_i$。

将属性 X 划分为 k 个区间，可以得到一个 m 行 k 列的矩阵 T

$$T=\begin{bmatrix}n_{11} & n_{12} & \cdots & n_{1k}\\ n_{21} & n_{22} & \cdots & n_{2k}\\ \vdots & \vdots & \cdots & \vdots\\ n_{m1} & n_{m2} & \cdots & n_{mk}\end{bmatrix}$$

T 的第 j 列 $T_j=[n_{1j}\ n_{2j}\cdots\ n_{mj}]^{\mathrm{T}}$，则有

$$T=[T_1,T_2,\cdots,T_k]$$

基于不确定测度，Zighed 提出了一种 Shannon 熵的准则函数 φ[3]，并且该准则函数必须满足以下几条原则：

(1)最小原则：如果每个离散区间的元素仅仅对应于同一种分类情况，则准则函数 φ 应该是最小的。（同定理 1）；

(2)最大原则：如果每个离散区间的元素对应了所有分类情况，则准则函数 φ 应该是最大的。（同定理 2）；

(3)设 T 是离散后获得的矩阵。如果用一个大于 1 的因子去扩大矩阵 T 的元素数值，准则函数 φ 的值必须也应该增大；

(4)对称原则：矩阵 T 中的列变换不影响准则函数的值；

(5)合并原则：如果两个连续的离散区间有相似的分布，即 T_j 和 T_{j+1} 成比例，那么这两个区间可以合并为一个区间，并且准则函数 φ 的值减小；

(6)独立性原则：如果合并了两个区间，则准则函数 φ 只与这两个进行合并的区间有关，与其他区间无关。

根据上述 6 条原则，Zighed 的准则函数定义为

$$\varphi(T)=\sum_{j=1}^{k}\alpha\frac{n_j}{n}\left(-\sum_{i=1}^{m}\frac{n_{ij}+\lambda}{n_j+m\lambda}\log_2\frac{n_{ij}+\lambda}{n_j+m\lambda}\right)+(1-\alpha)\frac{m\lambda}{n_j}$$

其中 λ,α 是两个可调的参数，用于控制连续属性 X 的离散区间数 k，一般取 $\lambda=1$，$\alpha=[0,1]$，用于调整离散点的个数。如果 $\lambda=0$，则该函数就是典型的 Shannon 熵表达式。文[3]中已证明该函数能够有效地对单个连续属性进行有效的离散。

2 基于信息熵的自动聚类算法

基于以上的 Shannon 熵的准则函数，可以有以下的自动聚类算法（FUSINTER 算法）：

(1)设样本集的连续属性 X 的取值按递增顺序排列为：$x_1<x_2<\cdots<x_{\tilde{n}}$，$\tilde{n}\leqslant n$；

(2)如果 X 的连续取值对应的分类相同，则这些值形成一个区间；

(3)如果 X 的同一取值对应的分类不同，则这个单独的值形成一个区间，它对应于一个混合的分类；

(4)经过过程(2)，(3)则可以把连续属性 X 的值初步划分为 k 个区间 $I_1,I_2,\cdots,I_k$，并且可以得到 $m\times k$ 阶的矩阵 T，$T=[T_1,T_2,\cdots,T_k]$。

(5)在 k 个区间 $I_1,I_2,\cdots,I_k$ 中寻找两个相邻区间 I_j,I_{j+1}，使得 $\varphi(T)-\varphi(T_1,\cdots,T_j+T_{j+1},\cdots,T_k)=\max_{j=1}^{k-1}(\varphi(T)-\varphi(T_1,\cdots,T_j+T_{j+1},\cdots,T_k))$，若 $\varphi(T)-\varphi(T_1,\cdots,T_j+T_{j+1},\cdots,T_k)>0$，则将这两个相邻区间 I_j,I_{j+1} 合并，并且令 $T=[T_1,\cdots,T_j+T_{j+1},\cdots,T_k]$，此时只有 $k-1$ 个区间了。

(6)根据 $k-1$ 个区间重复执行第(2)步到第(6)步，直到 $\varphi(T)$ 不再减少或 $k=1$ 为止。这样得到的最终区间个数即为该连续属性的最少离散区间。

由于 FUSINTER 算法只是针对单个连续属性，而实际信息系统中有多个连续属性。这就需要对多个连续属性分别使用 FUSINTER 算法进行离散，并且要求最终保证整个信息系统离散后是相容的和一致的，并且拥有较少的分割区间。对信息系统的总体相容性和离散程度可以通过 Shannon 熵的准则函数中的 α 值来调整，对于给定的信息系统，总存在一个最小的 α 值，使得所有的属性在 α 下离散后的信息系统是相容的。算法如下：

(1)设 $\gamma=1$；

(2)$\alpha=\gamma-\Delta\alpha$，$\Delta\alpha$ 为一个较小的步长；

(3)设条件属性的初始维数 $d=1$；

(4)利用 FUSINTER 算法对第 d 维条件属性进行离散，并对该条件属性利用量化参数进行量化；

(5)$d=d+1$，重复执行(3～5)步直到最后一个条件属性，形成量化的信息系统；

(6)检查量化的信息系统是否相容；

(7)若量化的信息系统相容，则令 $\gamma=\gamma-\Delta\alpha$，再重新从第(2)步执行；

(8)若量化的信息系统不相容，则令 $\alpha=\gamma$，转第(9)步；

(9)在 α 下，利用 FUSINTER 算法对全部条件属性进行离散，并对它们利用量化参数进行量化，最终得到相容的量化的信息系统。

该算法根据各个连续属性本身与决策属性之间的关系进行离散，最终得到的量化值个数随不同的条件属性可能不同。

3　实　　例

本文以干线飞机外形参数的变化趋势与其更新换代的关系来说明本文提出的连续属性离散化过程。本文选择国内外干线飞机外形设计数据建立决策表，见表 1。

表 1　国际部分干线飞机外形参数及其更新换代关系

序号	型号	翼展	展弦比	后掠角	机身长	机身高	机翼面积	更新换代
1	Tu-154	37.55	7	35	47.9	11.4	201.45	2
2	Tu-204	41.8	9.6	28	46.1	13.9	182.4	3
3	Tu-330	43.5	10.6	28	42	14	177.8	3
⋮	⋮	⋮	⋮	⋮	⋮	⋮	⋮	⋮
16	MD-90	32.87	9.6	24.5	46.51	9.33	112.3	3
17	B717-200	28.47	8.7	24.5	37.8	8.86	92.97	3

表 1 的决策表中条件属性为 $C=\{c_1,c_2,c_3,c_4\}$，决策属性为 $D=\{d\}$。其中 4 个条件属性均为连续属性，决策属性 D 为更新换代的代数，为了发现外形参数随时间的变化趋势，把决策属性 D 按照民航客机更新换代的标准标识为如下的离散属性

$$d=\begin{cases}1\text{（第一代旅客机：如 B707，涡喷发动机）}\\2\text{（第二代旅客机：尖峰式翼型，涡喷发动机）}\\3\text{（第三代旅客机：超临界翼型，涡扇发动机）}\end{cases}$$

对表 1 的各个连续条件属性应用本文方法进行离散，得到表 2 所示的量化值。条件属性离散化后的量化决策表见表 3。

表 2　条件属性量化参数表

属性代号	条件属性	条件属性量化值	
		1	2
c_1	翼展	(0，80)	
c_2	展弦比	(0，8.7)	[8.7，12]
c_3	后掠角	(0，40)	
c_4	机翼面积	(0，+∞)	

此为试读，需要完整PDF请访问：www.ertongbook.com